Drying-induced stress and deformation for clays : a numerical study of the problem

EINDHOVEN UNIVERSITY OF TECHNOLOGY
Department of Mathematics and Computing Science

RANA 99-30
October 1999

Drying-induced stress and deformation for clays: A numerical study of the problem

by

A. Hugget, W.J. Coumans, E.F. Kaasschieter

Reports on Applied and Numerical Analysis
Department of Mathematics and Computing Science
Eindhoven University of Technology
P.O. Box 513
5600 MB Eindhoven, The Netherlands
ISSN: 0926-4507

DRYING-INDUCED STRESS AND DEFORMATION FOR CLAYS : A NUMERICAL STUDY OF THE PROBLEM.

A. Hugget[1], W.J. Coumans[1] and E.F. Kaasschieter[2]

Eindhoven University of Technology

[1] Department of Chemical Engineering and Chemistry,

[2] Department of Mathematics and Computing Science,

P.O. Box 513, 5600 MB Eindhoven, THE NETHERLANDS

Email: a.w.b.hugget@tue.nl ; W.J.Coumans@tue.nl ; wsanrk@win.tue.nl

Correspondence concerning this article should be addressed to W.J. Coumans

Abstract

A brief overview of the drying-induced stress and strain problem is given, followed by a presentation of the governing equations and the finite element formulation. The mathematical formulation of mass transfer is based on the diffusion equation and an elastic model is used to compute drying-induced strain and stress. The von Mises cracking criterion is introduced in order to locate the area where danger for cracking occurs. The model is applied to the drying of a Kaolin brick with a square section. Danger for cracking is highest during the hours four first due to the important size of the clay sample. The cracking criterion reaches its peak value at the surface for the symmetry axes in 40 minutes and then decays slowly. Complementary examples are presented that demonstrate representative applications of such calculations.

Keywords: drying; diffusion; elasticity; shrinkage; cracking criteria; mathematical modelling.

INTRODUCTION

Drying is an operation which is present in important industrial processes involving minerals, agricultural products, forest and polymer. An example of a branch of industry, where drying plays an essential role in the production processes is the brick and tile manufacturing industry.

Shrinkage occurs during drying of many materials. It is pointed out that the shrinkage for clays is caused by particle slip into a more compact arrangement by Onoda *et al.* (1988). Moisture concentration gradients in

the material and corresponding gradients in the amount of shrinkage will lead to drying stresses. Controlling these stresses is important since they can lead to undesired deformations and/or cracks in the product. A correct description of the evolution of moisture concentration profiles in the material is complicated by the influence of shrinkage on mass transfer.

A review of papers dealing with drying-induced strain and stress has been made by Hasatani and Itaya (1996). Concerning the mechanical behaviour elastic or more complex models -in particular viscoelastic models- could be used, each one having its advantages and disadvantages.

Numerous papers deal with the simulation of drying-induced strain and stress using an elastic model. Jomaa (1991) assumed elastic properties to predict strain and stresses during gel drying. He concluded that the prediction of the final shape of the sample, by assuming the gel of being an elastic material, is not adequate and that the consideration of viscoelastic properties would most probably improve the shape prediction. Mrani *et al.* (1995) defined a theoretical model taking into account the simultaneous influence of mechanical and hygrometric actions to study the drying of a highly deformable two phases gel. Using this model for the non uniform drying of agar gel (Mrani et al., 1997) the numerical results showed a good agreement with experiments and the authors concluded that this kind of model could be used as a tool for improving the final quality of dried product. Brooke and Langrish (1997) studied an elastic model to simulate stresses and strains in the drying of Pinus radiata sapwood. Comparing with measured rupture stresses they observed that the elastic model over-estimates the stress level inside the timber. The authors concluded that their model is still useful to develop a better understanding of the effect of the board geometry and the drying conditions on the risk of cracking.

There have been published only a few papers on viscoelastic behaviour related to dehydration. Also the finite element technique has been extended to viscoelastic problems in only a few relatively simple cases which were based on the solution of integral equations in real time (Taylor and Chang, 1966; Srinata and Lewis, 1981). To overcome the difficulties of these solution schemes, Haghighi and Segerlind (1988a,b) developed a variational formulation for a finite element analysis of a viscoelastic sphere subjected to temperature and moisture gradients. Their numerical results were limited to an elastic solution since the viscoelastic properties for material being studied were not available. Irudayaraj and Haghighi (1993) proposed a theory and finite element formulation for the stress analysis of non-linear viscoelastic materials during drying. The history-dependent nature of viscoelastic behaviour required extensive computer storage

and time. Thus the only way to use efficiently their model was to define a computational scheme wherein the current solution depended only on solutions from the previous two time steps and to use a small number of elements (22).

From this literature survey it can be concluded that viscoelastic analysis is only limited to the simple problem, because the performance of new computers is still not sufficient for the problem, but also because it is quite difficult to propose an appropriate mechanical model and to obtain the necessary properties experimentally. For these reasons in most cases elastic models are used in order to arrive at a better understanding of the risk of cracking.

The main objectives of this research are 1) to develop the mathematical formulation of the problem and the way to solve it by using a Lagrangean frame and the finite element method; 2) to analyse the simulated drying behaviour; 3) to study the effect of different parameters such as diffusion coefficients on the drying and the mechanical behaviour.

In the first part of this paper the mathematical model is presented. A diffusion model is used to describe the moisture content evolution. Due to the lack of relevant mechanical properties for clays and the huge memory requirement to numerically solve the viscoelastic problem it is assumed that the clay behaves perfectly elastic. In a second part of this paper the corresponding finite element formulation is given. Different numerical problems and the way to solve them are studied. In the final part Kaolin drying is considered. Analysis of moisture content profiles, shape evolution and cracking criterion evolutions allow to understand where, when and why danger for cracking occurs. The effects of diffusion coefficients and of Young's modulus approximation are briefly discussed and some conclusions are drawn.

MATHEMATICAL MODELLING

Isothermal drying of clay can be modelled by equations expressing mass conservation of moisture and solid, together with a flux equation for moisture. This flux equation is essentially Darcy's law, where pressure and permeability depend on moisture content. A combination of these equations leads to a diffusion equation which is used in this study. This equation can be applied for systems with any degree of shrinkage (Coumans, 1987; Ketelaars, 1992).

The diffusion equation is supplemented with an expression for the deformation of clay due to gradients in moisture content. In this study, it is assumed that clay behaves like an elastic material, i.e. Hooke's law applies, where Young's modulus and Poisson's ratio depend on moisture content.

With the introduction of Lagrangean co-ordinates these equations can be transformed into a non-linear parabolic equation for the moisture conservation and a non-linear elliptic equation for the displacements that depends on the moisture content (Wigmans, 1994). The coupling between stresses and drying kinetics is very small (Ketelaars, 1992) and has been neglected. However, it should be realised that the diffusion coefficients determined from drying curves implicitly take into account this coupling.

Diffusion model

The description of mass transfer in porous media can be found in various literature references (e.g., (Whitaker, 1977)). In order to arrive at a practical, manageable model, simplification of the complete set of equations seems inevitable. A simplification most frequently encountered in drying is the so-called apparent diffusion coefficient. All mechanisms contributing to moisture transfer are lumped into a single diffusion coefficient. The model based on this assumption is often referred to as 'the' diffusion model. The diffusion model is a more phenomenological model, in contrast to mechanistic models. Different methods can be used to determine the diffusion coefficients from experimental data. The first technique is the measurement of drying curves (Coumans, 1987). The second experimental technique is the direct measurement of moisture profiles during the drying process. Example of non-destructive measurement methods are gamma or neutron attenuation methods (Ketelaars *et al.*, 1995) and nuclear magnetic resonance imaging (Pel, 1995; Kroes, 1998).

With respect to the diffusion model, the mass balances and flux equation that hold for the drying of a block of clay with any degree of shrinkage can be represented by the following equations (Coumans, 1987; Ketelaars, 1992):

- mass conservation of moisture :

$$\frac{\partial \rho_m}{\partial t} = -\nabla \cdot (\rho_m \mathbf{v}_m) , \tag{1}$$

- mass conservation of solid :

$$\frac{\partial \rho_s}{\partial t} = -\nabla \cdot (\rho_s \mathbf{v}_s) . \tag{2}$$

- flux equation for moisture :

$$\rho_m \mathbf{v}_m = \rho_m \mathbf{v}_s - \rho_s D(u) \nabla u , \tag{3}$$

where the moisture content is given by $u = \rho_m / \rho_s$.

The flux equation can be derived from mechanistic considerations by neglecting the effects of air transport, temperature gradients and gravity, and by assuming that the capillary pressure is a function of moisture content only (Puiggali *et al.*, 1988). Combining this set of equations leads to the form of the diffusion equation which is used in this study:

$$\frac{\partial u}{\partial t} + \mathbf{v}_s \cdot \nabla u = \frac{1}{\rho_s} \nabla \cdot (\rho_s D(u) \nabla u) \quad \text{in } \Omega_t, t>0, \tag{4}$$

where Ω_t is the time-dependent computational domain. This equation is supplemented with the initial condition

$$u(\mathbf{x},0) = u^0 , \quad \mathbf{x} \in \Omega_0, \tag{5}$$

and the boundary condition

$$-\rho_s D(u) \nabla u \cdot \mathbf{n} = J(u) \quad \text{on } \Omega_t, t>0, \tag{6}$$

where J(u) is the prescribed drying flux which can be found from the sorption isotherm and the external drying conditions.

Note that equations (4)-(6) are not complete, since Ω_t, ρ_s and $\mathbf{v}_s$ are unknown.

In order to make the computational domain constant, Lagrangean co-ordinates with respect to solid are used. Each clay particle will have a solid co-ordinate $\mathbf{z}=\mathbf{x}(0)$. Define the mapping $\mathcal{F}_t : \Omega \rightarrow \Omega_t$ by

$$\mathcal{F}_t(z)=x(t), \quad z\in\Omega,\ t\geq 0, \tag{7}$$

where $\Omega=\Omega_0$. Let $\mathcal{D}\mathcal{F}_t=\left[\nabla x\right]^T$ be the functional matrix of $\mathcal{F}_t$, and $\mathcal{J}_t=\det(\mathcal{D}\mathcal{F}_t)$ its Jacobian which represents the volume ratio of the continuum. It is clear that

$$x'(t)=v_s(x(t),t), \quad x\in\Omega_t,\ t>0, \tag{8}$$

and

$$\rho_s(x(t),t)=(\mathcal{J}_t(z))^{-1}\rho_s^0, \quad z\in\Omega,\ t\geq 0, \tag{9}$$

where $\rho_s^0=\rho_s(z,0)$, i.e. it is assumed that the initial solid concentration is constant.

It follows from (4)-(6), using (7)-(9) and the well-known transformation rules corresponding to the covariant and contravariant formalism (e.g., (Morse and Fesbach, 1953)), in solid co-ordinates **z**:

$$\begin{cases} \dfrac{\partial u}{\partial t}=\nabla\cdot(\widetilde{\mathbf{D}}(u)\nabla u) & \text{in } \Omega,\ t>0, \\ -\rho_s^0\mathbf{n}\cdot(\widetilde{\mathbf{D}}(u)\nabla u)=\widetilde{J}(u) & \text{on } \partial\Omega,\ t>0, \\ u(z,0)=u^0, & z\in\Omega, \end{cases} \tag{10}$$

where

$$\widetilde{\mathbf{D}}(u)=|\mathcal{D}\mathcal{F}_t|^{-1}D(u)|\mathcal{D}\mathcal{F}_t|^{-T}, \tag{11}$$

$$\widetilde{J}(u)=\mathcal{J}_t\left\||\mathcal{D}\mathcal{F}_t|^{-T}\mathbf{n}\right\|_2 J(u). \tag{12}$$

Note that (10) is still not complete, since $\mathcal{D}\mathcal{F}_t$ is unknown. In order to determine $\mathcal{D}\mathcal{F}_t$ the displacement due to mechanical stresses needs to be known.

Mechanical model

We assume that clays have perfectly elastic constitutions. Obviously this is an oversimplification of their actual mechanical behaviour. There are two important reasons for this simplification. First, it is very difficult to determine experimentally all the relevant mechanical properties to be used in more sophisticated constitutive models, especially since all these properties are functions of moisture content. Second, the numerical solution of these models is complicated. In addition to this it is assumed that the deformation due to stresses of clay is small, which is confirmed experimentally. Therefore, as a first approximation we will

use linear elastic constitutive equations. The resulting mechanical deformation holds instantaneously and therefore we omit the time t in the following equations.

Let $\mathbf{w}=\mathbf{x}-\mathbf{z}$ be the displacement, then $\mathcal{D}f_t = [\nabla \mathbf{x}]^T = \mathbf{I} + [\nabla \mathbf{w}]^T$. The total strain tensor is defined by $\varepsilon(\mathbf{w}) = (\nabla \mathbf{w} + [\nabla \mathbf{w}]^T)/2$. It is assumed that the total strain is the sum of the elastic strain due to the stress and the dilatation due to shrinkage, i.e.

$$\varepsilon(\mathbf{w}) = \varepsilon^e + \varepsilon^s. \tag{13}$$

Since the material is assumed to be isotropic, the elastic strain can be determined from Hooke's law:

$$\varepsilon^e = \frac{1+\nu(u)}{E(u)}\left(\sigma - \frac{\nu(u)}{1+\nu(u)}\mathrm{tr}[\sigma]\mathbf{I}\right). \tag{14}$$

The dilatation due to shrinkage is assumed to be isotropic, i.e.

$$\varepsilon^s = \varepsilon^s \mathbf{I}. \tag{15}$$

It is also assumed that shrinkage only depends on moisture content. Define the prescribed shrinkage factor

$$\psi_s(u) = J_t \le 1, \tag{16}$$

then $\det(\mathbf{I}+\varepsilon^s)=(1+\varepsilon^s)^3=\psi_s(u)$ and thus

$$\varepsilon^s = \varepsilon^s(u) = |\psi_s|^{1/3} - 1. \tag{17}$$

Note that the shrinkage factor $\psi_s(u)$ is the equilibrium relation between the specific volume (m^3/kg dry solid) of a piece of clay and its moisture content.

From (13)-(15) it follows that

$$\varepsilon(\mathbf{w}) = \frac{1+\nu(u)}{E(u)}\left(\sigma - \frac{\nu(u)}{1+\nu(u)}\mathrm{tr}[\sigma]\mathbf{I}\right) + \varepsilon^s(u)\mathbf{I}, \tag{18}$$

and, inverting (18),

$$\sigma = \frac{E(u)}{1+\nu(u)}\left(\varepsilon(\mathbf{w}) + \frac{\nu(u)}{1-2\nu(u)}\mathrm{tr}[\varepsilon(\mathbf{w})]\mathbf{I}\right) - \frac{1+\nu(u)}{1-2\nu(u)}\varepsilon^s(u)\mathbf{I}. \tag{19}$$

Neglecting gravity and accelerations forces, the momentum balance law is

$$[\nabla \cdot \sigma]^T = 0. \tag{20}$$

Assuming no external forces, the boundary condition for (19)-(20) is

$$\sigma \mathbf{n} = 0. \tag{21}$$

Define the Lamé coefficients $\lambda(u)$ and $\mu(u)$, and the bulk modulus $K(u)$, by

$$\lambda(u) = \frac{E(u)\nu(u)}{(1-2\nu(u))(1+\nu(u))}, \quad \mu(u) = \frac{E(u)}{2(1+\nu(u))}, \quad K(u) = \frac{E(u)}{3(1-2\nu(u))},$$

then (18)-(21) result in

$$\begin{cases} \nabla \cdot \left[\lambda(u)\mathrm{tr}(\varepsilon(w))\mathbf{I} + 2\mu(u)\varepsilon(w)\right] = \nabla \cdot \left[3K(u)\varepsilon^s(u)\mathbf{I}\right] & \text{in } \Omega, \\ \lambda(u)\nabla \cdot w\mathbf{n} + 2\mu(u)\varepsilon(w)\mathbf{n} = 3K(u)\varepsilon^s(u)\mathbf{n} & \text{on } \partial\Omega. \end{cases} \tag{22}$$

Coupling of the complete set of equations

The complete set of equation (10) and (22) can be simplified by neglecting the elastic strain with respect to the shrinkage dilatation, which means that the deformation due to stress is much smaller than the deformation due to shrinkage, resulting into

$$\mathcal{D}f_1 = [\psi_s(u)]^{1/3}\mathbf{I}. \tag{23}$$

This approximation is only used to solve the diffusion problem. It then follows from (10)-(12) that

$$\begin{cases} \dfrac{\partial u}{\partial t} = \nabla \cdot (|\psi_s(u)|^{-2/3} D(u)\nabla u) & \text{in } \Omega,\ t > 0, \\ -\rho_s^0 \mathbf{n} \cdot (|\psi_s(u)|^{-2/3} D(u)\nabla u) = [\psi_s(u)]^{2/3} J(u) & \text{on } \partial\Omega,\ t > 0, \\ u(z,0) = u^0, & z \in \Omega \end{cases} \tag{24}$$

Model limitations

With the help of the precedent model it is possible to calculate the moisture concentration distribution in the clay body, and the connected stresses. Stresses will lead to additional deformations on top of the deformation due to shrinkage. In principle these stress-induced deformations have to be taken into account in the drying kinetics model. If this effect is to be included in the model it would lead to a coupling of the kinetics model and the mechanical model, which complicates the numerical solution of the problem. It is therefore assumed that the deformations due to stresses are small compared to the deformations due to shrinkage. Note that this restriction can be verified once both deformations are calculated with the stress

model. The mechanical behaviour of the material is implicitly coupled with the kinetic model via the experimental diffusion coefficients. One of the advantages of this lumped coefficient is to take into account all mechanisms contributing to moisture content transfer (as the mechanical behaviour of the material). This advantage could be at the same time a disadvantage if we try to understand the mechanisms and their influence. For example in using this model it is still impossible to make a sensitivity study to understand the effect of the mechanical material behaviour on mass transfer.

FINITE ELEMENT DISCRETISATION

The numerical solution is obtained using a standard finite element package (SEPRAN, see (Segal, 1998)) which is adapted for the problem studied here. This code can be used for one-dimensional, two-dimensional or three-dimensional problems. The used Finite Element Method (FEM) is standard and is not exposed in details. The problem has to be written in a weak formulation, the so-called variational form. The block-shaped domain Ω is supposed to be divided in a collection of block-shaped subdomains, called elements. The elements have to be a partition of the computational domain. For the time discretisation the time interval $]0,T]$, $T>0$, has to be divided into a partition given by

$$0=t_0<t_1< \ldots <t_N=T$$

for some natural number N. Let $\Delta t_n=t_n-t_{n-1}$, $n=1,\ldots,N$, be the time steps. The system of equations is discretised in time by the backward Euler method with frozen coefficients. The resulting sparse linear systems are solved by preconditioned conjugate gradients.

The FEM applied to the diffusion problem

Concerning the diffusion problem the solution $u(\cdot,t_n)$, $n=1,\ldots,N$, of (24) is approximated by a function $u_h^n \in V_h$. Solving the diffusion problem requires to approximate the time derivative. For the discretisation of the time derivative we can use an explicit or an implicit method. An explicit method is conditionally stable and an implicit method can be unconditionally stable. The backward Euler implicit method is used in this paper. For the derivation of the variational problem the Sobolev space of scalar functions V is used. Let V_h be the finite-dimensional subspace of V consisting of piecewise linear functions defined on each element.

Multiplying the diffusion equation by a test function $v_h \in V_h$, integrating over the region Ω and applying the divergence theorem, the discrete approximate function u_h^n is defined to be the solution of

$$\frac{1}{\Delta t_n}\int_\Omega (u_h^n - u_h^{n-1})v_h dz + \int_\Omega (\tilde{\mathbf{D}}(u_h^n)\nabla u_h^n)\cdot\nabla v_h dz$$
$$= \frac{1}{\rho_s^0}\int_{\partial\Omega} \tilde{J}(u_h^n)v_h ds, \quad \forall v_h \in V_h, n = 1,\ldots,N, \tag{25}$$

$$u_h^0(z) = u^0, \quad z \in \Omega, \tag{26}$$

(see (Douglas and Dupont, 1970) and (Carey and Oden, 1984)).

Let $u_h^n = \sum_{i=1}^{N} u_i^n \varphi_i$, where φ_i are the basis functions of V_h. Successive choice of the test functions $v_h = \varphi_i$, i=1,2,....,M, implies the equivalence of (25) with the system of non-linear equations

$$(\mathbf{M} + \Delta t_n \mathbf{S}^n)\mathbf{u}^n = \mathbf{M}\mathbf{u}^{n-1} + \Delta t_n \mathbf{F}^n, \tag{27}$$

where

$$M_{ij} = \int_\Omega \varphi_j \varphi_i dz, \quad i,j = 1,2,\ldots,M, \tag{28}$$

$$S_{ij}^n = \int_\Omega (\tilde{\mathbf{D}}(u_h^n)\nabla\varphi_j)\cdot\nabla\varphi_i dz, \quad i,j = 1,2,\ldots,M, \tag{29}$$

$$F_i^n = \frac{1}{\rho_s^0}\int_{\partial\Omega} \tilde{J}(u_h^n)\varphi_i ds, \quad i = 1,2,\ldots,M, \tag{30}$$

and $\mathbf{u}^n$ is the solution vector. The matrix $\mathbf{M}$ is called the mass matrix, the matrix $\mathbf{S}^n$ is called the stiffness matrix and the vector $\mathbf{F}^n$ is the right-hand side vector. The matrix $\mathbf{M} + \Delta t_n \mathbf{S}^n$ is sparse and symmetric positive definite because the diffusion coefficient $\mathbf{D}$ is positive. This non-linear problem is hard to solve because the diffusion coefficient and the prescribed drying flux will be evaluated by the solution to be computed. An easy way to linearise this non-linear problem is to 'freeze' the coefficients. This means that the diffusion coefficient and the prescribed drying flux will be evaluated with the solution at the preceding time level. In this case the matrix equations to be solved read

$$(\mathbf{M} + \Delta t_n \mathbf{S}^{n-1})\mathbf{u}^n = \mathbf{M}\mathbf{u}^{n-1} + \Delta t_n \mathbf{F}^{n-1}. \tag{31}$$

An adaptive time step procedure is used. As long as the prescribed drying flux is nearly constant near the whole boundary the time step size can be chosen large. The slope of the prescribed drying flux for low moisture contents is extremely steep. When this occurs, the time step has to be small.

The way of linearising causes a numerical problem. By freezing coefficients the prescribed drying flux is evaluated on a preceding time level and therefore is too high. The time steps for low moisture contents at the boundary are smaller than necessary. Since the small time steps are due to the extreme slope of the prescribed drying flux for low moisture contents, it is necessary to compute the prescribed drying flux implicitly. For this problem, an iterative solution procedure does not converge. It seems more appropriate to prescribe a Robin boundary condition (mixed boundary condition) instead of a Neumann condition. The Neumann boundary condition from (24) in material co-ordinates can be written as the Robin condition

$$\rho_s^0 \, \mathbf{n} \cdot (\tilde{\mathbf{D}}(u) \nabla u) + \tilde{j}(u) u = 0, \tag{32}$$

where $\tilde{j}(u) = \tilde{J}(u)/u$. By using the Robin boundary condition and by freezing the coefficients of $\tilde{j}(u)$, the matrix equation to be solved reads

$$(\mathbf{M} + \Delta t_n \mathbf{B}^{n-1} + \Delta t_n \mathbf{S}^{n-1}) \mathbf{u}^n = \mathbf{M} \mathbf{u}^{n-1}, \tag{33}$$

where

$$B_{ij}^{n-1} = \frac{1}{\rho_s^0} \int_\Omega \tilde{j}(u_h^{n-1}) \varphi_j \varphi_i \, dz, \quad i, j = 1.2, \ldots, M. \tag{34}$$

Taking into account (26), (33) can be solved very efficiently by the preconditioned conjugate gradient method (see, e.g., (Saad, 1996)).

The FEM applied to the stress problem

Time discretisation for the stress problem is necessary because the stress depends on the moisture content, i.e. the solution of the diffusion problem. The approximation of the solution $w(.,t_n)$ at time t_n will be denoted as $\mathbf{w}_h^n$. For the derivation of the variational problem the Sobolev space of vectorial functions - called **V**- is used. Let $\mathbf{V}_h$ be again the finite-dimensional subspace of **V** consisting of piecewise linear functions defined on each element. Since the conservation law of momentum does not contain any time derivatives the discretised variational formulation reads: Find $\mathbf{w}_h^n \in \mathbf{V}_h$ such that

$$\begin{aligned} &\int_\Omega \left[\lambda(u_h^n)\nabla\cdot\mathbf{w}_h^n\ \nabla\cdot\mathbf{v}_h + 2\mu(u_h^n)\varepsilon(\mathbf{w}_h^n):\varepsilon(\mathbf{v}_h)\right]dz \\ &\quad = 3\int_\Omega K(u_h^n)\varepsilon^*(u_h^n)\nabla\cdot\mathbf{v}_h\,, \qquad \forall \mathbf{v}_h \in \mathbf{V}_h. \end{aligned} \tag{35}$$

Let $\mathbf{w}_h^n = \sum_{i=1}^{K} w_i^n \chi_i$, where $\{\chi_i\}_{i=1}^{K}$ are the basis functions of $\mathbf{V}_h$. Choosing the test functions $\mathbf{v}_h = \chi_i$, i=1,2,...,K, successively, (35) is equivalent with the matrix equation

$$\mathbf{A}(u_h^n)\mathbf{w}^n = \mathbf{b}(u_h^n), \tag{36}$$

where

$$A_{ij}(u_h^n) = \int_\Omega \left[\lambda(u_h^n)\nabla\cdot\chi_j\ \nabla\cdot\chi_i + 2\mu(u_h^n)\varepsilon(\chi_j):\varepsilon(\chi_i)\right]dz, \quad i,j = 1,2,...,K, \tag{37}$$

$$b_i(u_h^n) = 3\int_\Omega K(u_h^n)\varepsilon^*(u_h^n)\nabla\cdot\chi_i\ dz, \ i = 1,2,...,K, \tag{38}$$

and $\mathbf{w}^n$ is the solution vector. The matrix **A** is symmetric and positive definite, because the Lamé parameters are positive. This means that the matrix equation (36) has a unique solution.

By solving the variational formulation (36) in the beginning of the drying process the stresses at the boundary are still calculated poorly. In fact the Lamé parameters and the derivatives of the displacements have to be computed for the calculation of stresses. In the beginning of the drying process the displacements at the boundary of the clay will be large, whereas the displacements inside are small. Therefore, the derivatives of the displacements, the Lamé parameters and their products are large. This involves that in the beginning of the drying the stresses at the boundary are calculated poorly. Since the stresses are calculated from derivatives of the displacements the stresses are a derived quantity. Therefore,

it is probably better to solve the stress problem by the mixed finite element method (see, e.g., (Brezzi and Fortin, 1991)) because besides the displacements the stresses can be computed explicitly using this approach.

Since the mechanical model holds instantaneously -because the model is elastic-, (36) only need to be solved for the time on which the displacements and stresses are of interest.

KAOLIN DRYING

Physical properties

As an example, the drying of a Kaolin clay -which is used in the fine ceramics industry- at 25°C is considered. The initial moisture content u_0 of the clay is 0.4 and the initial solid concentration of solid $\rho_s^0 = 1234.6$. The following data are relevant for this type of product.

The experimental diffusion coefficients of Kroes (1998) for both shrinking and non-shrinking stages are used (see figure 1). The diffusion coefficients are approximated using Artificial Neural Networks (ANN). On the one hand we can notice the minimum in the diffusion coefficients for $u \approx 0.03$. This minimum is due to the fact that the rate of diffusion for water vapour is higher than the rate of diffusion for liquid water. On the other hand, for moisture contents above the shrinkage limit the diffusion coefficient tends to decrease with increasing moisture content. During drying of a shrinking medium the permeability will decrease because of a decreasing porosity. However, due to electrochemical effects the effect of the liquid pressure (also called osmotic suction pressure) on D will increase in colloidal systems, as can be found in literature (Newitt and Coleman, 1952). Apparently the latter mechanism is dominant here.

Experimental determination of the shrinkage factor $\psi_s(u)$ obtained by Ketelaars (1992) is used in this paper.

$$\psi_s(u) = \begin{cases} \dfrac{0.41 + u}{0.81} & \text{if } u \geq u_{lim}, \\ \dfrac{0.68}{0.81} & \text{if } 0 \leq u \leq u_{lim}, \end{cases} \tag{39}$$

where u_{lim} is the moisture content at shrinkage limit. Considering the Kaolin clay, $u_{lim}=0.27$.

The prescribed drying flux J(u) is given by (Ketelaars, 1992)

$$J(u) = \frac{16 \cdot 10^{-4}}{\pi} \arctan(1.5 \cdot 10^{2} u). \tag{40}$$

Prescribed drying flux and shrinkage factor as functions of moisture content are given in figure 2.

Considering the mechanical behavior of the Kaolin clay, the experimental Young's modulus E as a function of moisture content obtained by Ketelaars (1992) is used (figure 3). This function is approximated using ANN. The following non-continuous approximation given by Ketelaars (1992) can also be used

$$E(u) = \begin{cases} 3 \cdot 10^{7-12\,o(u-u_{lim})} & \text{if } u \geq u_{lim}, \\ 3 \cdot 10^{7} & \text{if } 0 \leq u \leq u_{lim}. \end{cases} \tag{41}$$

We will show the differences involved by the use of these two kinds of approximation. The Poisson's ratio ν is constant and equal to 0.45.

Problem configuration

In figure 4 a sketch is given of the geometry under consideration (a brick with a cross-section of 10 × 10 cm). It is assumed that no drying occurs at the ends of the bar and therefore no moisture concentration will be present along the z-axis. In such a situation a two-dimensional plane-stress analysis can be made of a cross-section of the brick. In addition to this, drying occurs with equal initial drying fluxes at the other boundaries. As a result of symmetry only the upper right quarter of the two-dimensional cross-section need to be considered (figure 4). On the two "symmetry" faces the following homogeneous boundary conditions are imposed

$$\left.\begin{aligned} \frac{\partial u}{\partial n} &= 0, \\ \mathbf{w} \cdot \mathbf{n} &= 0, \end{aligned}\right\} \quad t > 0. \tag{42}$$

The resulting computational domain is subdivided into 8100 rectangular elements, such that the mesh is refined along the external faces. A large number of elements is necessary to obtain a sufficient accuracy. In fact this kind of problem involves a strong evolution of stresses between the shrinkage and the non-shrinkage zones. An evolutionary mesh (i.e. with a larger number of element near this moving area) should be useful to decrease the number of elements.

The moisture content is approximated from (33), where the time-steps Δt_n are chosen by some automatic time-stepping procedure. From this approximation, solving (36), the displacement $\mathbf{w}$ and the stress σ are computed.

Moisture content evolution

As a first result moisture content along profile r for different drying times are given in figure 5. The left sides of the following figure (i.e. r=0 m) correspond to the centre of the clay brick and the right sides (i.e. r=0.07 m) correspond to the upper right corner point. We observe that in the beginning of the drying process the moisture content decreases fast, especially in the corner where the evaporation surface is important. For low moisture contents at the boundary the prescribed drying flux becomes very small, so that hardly any water can evaporate anymore. Therefore, it takes a long time before the interior of the clay is dry. We clearly notice from this figure a drying front moving inside. This is characteristic for drying behaviour and is due to the minimum in the diffusion coefficients according to curve 1. The presence of a minimum is related to the vapour diffusion mechanism, which may enhance the moisture flux considerably. Below a certain moisture content the vapour pressure is reduced according to the sorption isotherm. Since moisture gradients are present this will lead to a vapour pressure gradient in the gas phase. Small differences in liquid moisture concentration will cause significant vapour pressure gradients. The vapour is quickly transported to the surface and a receding drying front occur. From this figure we can also notice a slope break for u≅0.1. This break is due to the form of the diffusion coefficient curve: D increases strongly for a moisture content varying from 0.03 to 0.1, and is nearly constant from 0.1 to 0.4. The slope break for the diffusion coefficient is related to the slope break in the moisture profile curve.

Evolution of the shape

The evolution of the boundary surface y (see figure 4) is given in figure 6. We observe that in the beginning of the drying process the moisture content decreases faster in the corner which involves a larger strain. At the end of the drying the sample shape is the same as at the beginning, but the dimensions are smaller. This result is apparent since an elastic mechanical model is used. For a more complex shape at the end of the drying a viscoelastic or an elastoplastic model should be developed.

Stress analysis

The conditions that lead to failure can be determined by using a specific failure criterion. The trace of the Cauchy stress tensor is proportional to the hydrostatic pressure (dilatational forces) which does not cause cracking in the clay brick. In order to prevent cracking the deviation from the hydrostatic pressure and the

shear stresses have to be controlled. Therefore we consider the deviator $\overline{\sigma}$ of the Cauchy stress tensor defined as follows:

$$\overline{\sigma} = \sigma - \frac{1}{3}\mathrm{tr}(\sigma)\,\mathbf{I}. \tag{43}$$

Cracking in the brick has to be independent of the choice of the coordinate basis. Therefore a criterion for cracking must depend on the invariant of $\overline{\sigma}$. Since the first invariant of $\overline{\sigma}$ (i.e., $\mathrm{tr}(\overline{\sigma})$) is zero, the criterion can only depend on the second and the third invariant of $\overline{\sigma}$. In this study the well-known Huber-von Mises yield criterion proposed for problems in which frictions are not important (see, e.g., (Shigley and Mischke, 1989; Irudayaraj et al., 1993b)) will be used for determining the positions where danger for cracking occurs. This criterion depends only on the second invariant of $\overline{\sigma}$ (i.e., $-\frac{1}{2}\mathrm{tr}[\overline{\sigma}^2]$), and states that in order to prevent cracking in the brick we have to satisfy the condition

$$\sqrt{\frac{3}{2}\mathrm{tr}[\overline{\sigma}^2]} < Y. \tag{44}$$

where Y is the yield stress. The yield stress represents the stress where the material under uniaxial tension starts to deform plastically. The yield stress for Kaolin clay as a function of moisture content is determined experimentally by Ketelaars (1992) and can be fitted by

$$Y(u) = \begin{cases} 5\cdot 10^5, & \text{if } 0 \le u \le u_{lim}, \\ 5\cdot 10^{5-14.8(u-u_{lim})}, & \text{if } u \ge u_{lim}. \end{cases} \tag{45}$$

For moisture contents below the shrinkage limit the yield stress is constant. An explanation is that for moisture contents below the shrinkage limit the pores of the clay are not completely filled with water anymore, so that in this case the stiffness of the clay is independent of the moisture content.

In order to study the positions where stresses are important and danger for cracking occurs we will follow the temporal evolution for different section of the square sample of $\sqrt{\frac{3}{2}\mathrm{tr}[\overline{\sigma}^2]}$ (called the stress criterion) and of $Y-\sqrt{\frac{3}{2}\mathrm{tr}[\overline{\sigma}^2]}$ (called the cracking criterion) corresponding to the Huber-von Mises yield criterion. Note that danger for cracking occurs only if the cracking criterion is negative.

In figure 7a the stress criterion for the section x is given for different drying times. At the beginning of the drying the stress criterion increases strongly at the external boundary surface. To be more precise the stress

criterion increases at the surface until the moisture content becomes lower than the shrinkage limit moisture content (u_{lim}=0.27). After this critical moisture content the stress criterion decreases slowly. The largest stresses occur at the surface of the sample and for approximately t=2200s.

From figure 7b showing the stress criterion evolution along profile r, it follows that the temporal evolution is quite different. This is due to the configuration of this area: while the precedent case is nearly a one-dimensional configuration, this case is really a two-dimensional configuration with a more important drying rate involved from the second drying surface. The behaviour becomes then more complex. We can observe for each drying time a break slope and a maximum exactly for the distance r where the moisture content is equal to 0.27. The pressure and tension are maximal near the contour $u=u_{lim}$ because here, the influence of shrinkage and no shrinkage is maximal. But the value of this maximum increases from the beginning of the drying to t=6000s and then decreases more slowly. For this section the maximum stress occurs later and inside the sample. Stresses are not important at the surface due to the high drying rate involved by the configuration.

In figure 8 the cracking criterion evolution along profiles x and r is represented. The lower this criterion is, the more important the danger for cracking will be. We can note that for this problem configuration (i.e. sample geometry, drying conditions, etc.) the model predicts an important risk of cracking. This is due to the large dimensions of the sample which involves important moisture content and strain gradients. Furthermore, in comparison to a viscoelastic or a viscoplastic model, the elastic model generally overestimates the danger of cracking.

The largest danger occurs for the profile x at the surface from 1000s to 4000s. Due to the sample configuration corners dry very quickly which involves important strains. Thus large tensile stresses appear at the surface of each symmetry axis (e.g., for the profile x and x=0.05m) while the moisture content is still high (and thus the yield stress value is very low). Combining this large tensile stress with the low yield stress the danger for cracking becomes really important. Inside the sample the risk is less important and appears from 5000s to 16000s.

Figure 9 shows the evolution of the stress criterion maximum and of the cracking criterion minimum considering the global sample. The risk of cracking exists at the beginning of the drying, is really important from 1000s to 4000s with a maximum for t=2200s, and disappears after 17000s. The maximum of danger occurs exactly when the stress criterion is the largest.

Diffusion coefficients effect

As a first numerical experiment we can try to understand better the effect of the diffusion coefficients. Figure 10 compares the results obtained using the ANN diffusion coefficients and a constant one equal to $2.35\,10^{-8}$ m^2s^{-1} (which is the average of the ANN diffusion coefficients for u varying from 0.2 to 0.4). By comparing these results a different behaviour can be noticed. On the one hand, using a constant diffusion coefficient the clay sample dries faster (particularly for $u \leq u_{lim}$) and the drying front doesn't appear. On the other hand, we can note that the difference for the boundary displacement and for the stress criterion profile is small. Other numerical experiments show that diffusion coefficients only influence the mechanical behaviour for the range of moisture content from 0.4 to 0.2. If we are interested in the mechanical problem –e.g. to predict when and where the risk for cracking is maximum- the diffusion coefficients have to be defined with accuracy only for high moisture content. In this studied case a constant diffusion coefficient appears to be sufficient to understand mechanical phenomena.

Young's modulus approximation effect

The second numerical experiment (figure 11) allows to compare the use of the continuous approximation of the Young's coefficient (using ANN) and the non-continuous one (defined by Ketelaars (1992)), see figure 3. Moisture content profiles are the same and are not represented in this figure. The boundary displacement and the stress criterion are quite different using these two kinds of approximation. The larger difference appears for the stress criterion (curves b and c): the discontinuity of E involves higher values for the stress criterion. (This strong effect is the same considering the cracking criterion but is not presented in the figure). Furthermore the use of the non-continuous approximation of E affects quantitatively and qualitatively the maximum values of the stress criterion for the global sample: the danger for cracking is more important and its maximum appears roughly and for a shorter drying time. A good approximation of the Young's modulus appears to be very important and necessary to approximate accurately drying-involved strain and stress.

CONCLUSIONS

In this paper a mathematical model has been developed in order to represent the drying of clays. A diffusion model is used to obtain the moisture content evolution and an elasticity model allows to compute displacements and stresses. The problem is solved by the finite element method.

Numerical experiments for kaolin drying are considered. These results allow a better understanding of the positions in the clay brick and the time interval where danger for cracking occur. The largest danger is located at the surface of the sample near the symmetry axes for t≈2200s. Furthermore the pressure and tension are large near the contour $u=u_{lim}$ due to the influence of shrinkage and no shrinkage phenomena. The danger for cracking is important for the studied case due to the large dimension of the sample. Furthermore, it may be expected that the inclusion of visco-elastic or visco-plastic strains would decrease the danger of cracking, in other words the use of an elastic model yields.

Two numerical experiments are considered in order to obtain better understanding of the effect of both diffusion coefficient and Young's modulus. It follows that the type of moisture dependence of the diffusion coefficient at low moisture content with respects to the displacements and the stress criterion is not important. Considering two different ways to approximate experimental values for the Young's modulus, numerical results are very different. A non-continuous approximation involves larger values for the stress criterion and overestimates the danger for cracking. A representative definition of Young's modulus is one of the more important steps in order to obtain a realistic model useful to increase the final product quality.

NOTATION

D	diffusion coefficient, $m^2 s^{-1}$
$\tilde{D}$	diffusion coefficient in the Lagrangean frame, $m^2 s^{-1}$
E	Young's modulus, $N m^{-2}$
J	prescribed drying flux, $kg m^{-2} s^{-1}$
$\tilde{J}$	prescribed drying flux in the Lagrangean frame, $kg m^{-2} s^{-1}$
K	bulk modulus, $N m^{-2}$
t	time, s
T	temperature, °C
u	solid based moisture content, (kg water) (kg ds)$^{-1}$
v	velocity, $m s^{-1}$
w	displacement, m
x	place coordinate, m
z	solid based place coordinate, m

Greek letters

ε	strain
λ	Lamé coefficient, $N m^{-2}$

μ	Lamé coefficient, N m^{-2}
ν	Poisson's ration
ρ	concentration, kg m^{-3}
σ	stress, N m^{-2}
ψ_s	shrinkage function

Subscripts

m	moisture
s	solid

Superscript

e	elastic
s	shrinkage
0	initial, at t = 0 s

REFERENCES

Brezzi, F. and Fortin, M., 1991. Mixed and Hybrid Finite Element Methods. Springer, New York.

Brooke, A.S. and Langrish, T.A.G., 1997. The simulation of stresses and strains in the drying of *Pinus radiata* sapwood: the effects of board geometry. Computers chem. Engng., 21(11): 1271-1281.

Carey, G.F. and Oden, J.T., 1984. Finite Elements. Volume III : Computational Aspects. Prentice-Hall, Englewood Cliffs.

Coumans, W.J., 1987. Power Law Diffusion in Drying Processes. Ph.D. thesis, Eindhoven University of Technology, The Netherlands.

Douglas, Jr.J. and Dupont, T., 1970. Galerkin methods for parabolic equations. SIAM Journal on Numerical Analysis, 7 : 575-626.

Haghighi, K. and Segerlind, L.J., 1988a. Failure of biomaterials subjected to temperature and moisture gradients using the finite element method: I – Thermo-hydro Viscoelasticity. Trans. of the ASAE, 31(3): 930-937.

Haghighi, K. and Segerlind, L.J., 1988b. Failure of biomaterials subjected to temperature and moisture gradients using the finite element method: II – Stress analysis of an isotropic sphere during drying. Trans. of the ASAE, 31(3): 938-946.

Irudayaraj, J., Haghighi, K. and Stroshine, R., 1993a. Stress analysis of viscoelastic materials during drying: I – Theory and finite element formulation. Drying Tech., 11(5): 901-927.

Irudayaraj, J., Haghighi, K. and Stroshine, R., 1993b. Stress analysis of viscoelastic materials during drying: II – Application to grain Kernels. Drying Tech., 11(5): 929-959.

Jomaa, W., 1991. Séchage de matériaux fortement déformables: Prise en compte de la vitesse de retrait. Ph.D. thesis, Bordeaux I University, France.

Ketelaars, A.A.J., 1992. Drying Deformable Media : Kinetics, Shrinkage and Stresses. Ph.D. thesis, Eindhoven University of Technology, The Netherlands.

Ketelaars, A.A.J., Pel, L., Coumans, W.J. and Kerkhof, P.J.A.M., 1995. Drying kinetics: A comparison of diffusion coefficients from moisture concentration profiles and drying curves. Chemical Engineering Science, 50(7): 1187-1191.

Kroes, B., 1998. Transport Phenomena During Drying of Clays and Mixtures of Clays. Ph.D. Thesis, Eindhoven University of Technology, The Netherlands.

Morse, P.M. and Feshbach, H., 1953. Methods for Theoretical Physics. McGraw-Hill, New-York.

Mrani, I., Bénet, J.C. and Fras, G., 1995. Transport of water in a biconstituent elastic medium. Drying Tech., 48(10): 717-721.

Mrani, I., Bénet, J.C, Fras, G. and Zrikem, Z., 1997. Two dimensional simulation of dehydration of a highly deformable gel : Moisture content, stress and strain fields. Drying Tech., 15(9): 2165-2193.

Newitt, D.M. and Coleman, M., 1952. The mechanisms of drying of solids. Part 3, the drying characteristics of China clay. Transactions of the Institution of Chemical Engineers, 30: 28-45.

Onoda, G., Liniger, E.G. and Janney, M.A., 1988. Dilatancy and Plasticity in Ceramic Particulate Bodies, Ceram. Trans. I (Ceramics Powder Sci. II). Eds. Messing, G.L., Fuller, E.R. and Hausner, H., pp. 611-623.

Pel, L., 1995. Moisture Transport in Porous Building Materials. Ph.D. Thesis, Eindhoven University of Technology, The Netherlands.

Puiggali, J.R., Quintard, M. and Withaker, S., 1988. Drying granular porous media : gravitational effects in the isenthalpic regime and the role of diffusion models. Drying Tech., 6(4): 601-629.

Saad, Y., 1996. Iterative Methods for Sparse Matrices. PWS, Boston.

Segal, G., 1998. Sepran User's Manual. Leidschendam.

Shigley, J.E. and Lewis, R.W., 1989. Mechanical Engineering Design. Mc Graw-Hill book company, New York.

Srinata, H.R. and Lewis, R.W., 1981. A finite element method for thermo viscoelastic analysis of plane problems. Computer methods in applied mechanics and engineering, 25: 21-33.

Taylor, R.L. and Chang, T.Y., 1966. An approximate method for thermoelastic stress analysis. Nuclear Engineering Design, 4: 21-28.

Wigmans, A., 1994. A model for the Drying Process of Clay. Master's Thesis, Eindhoven University of Technology, The Netherlands.

Whitaker, S., 1977. Simultaneous Heat, Mass and Momentum Transfer in Porous Media : A Theory of Drying. Adv. Heat Mass Trans., 13: 110-203.

FIGURES

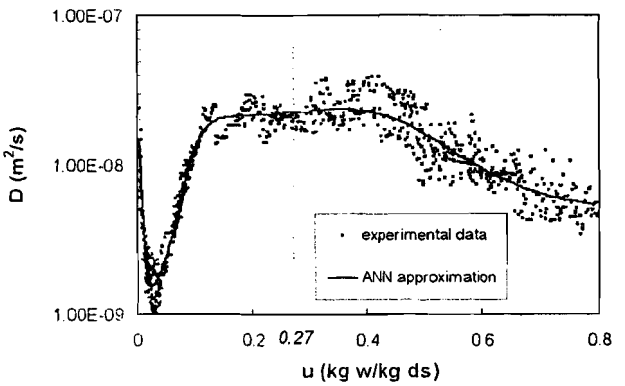

Fig. 1. Approximation of the experimental diffusion coefficients using an Artificial Neural Network.

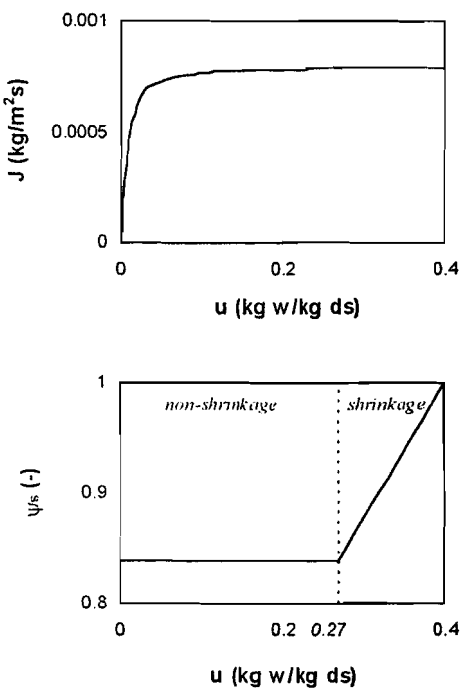

Fig. 2. Prescribed drying flux and shrinkage factor as functions of moisture content.

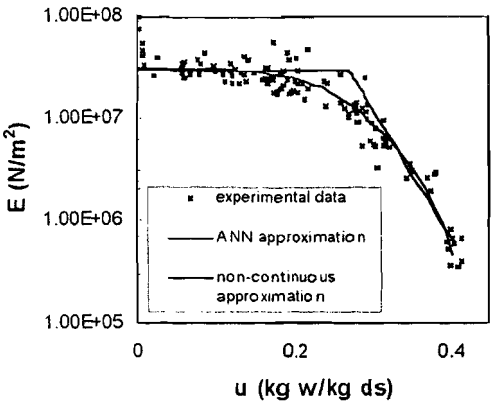

Fig. 3. Young's modulus as a function of moisture content.

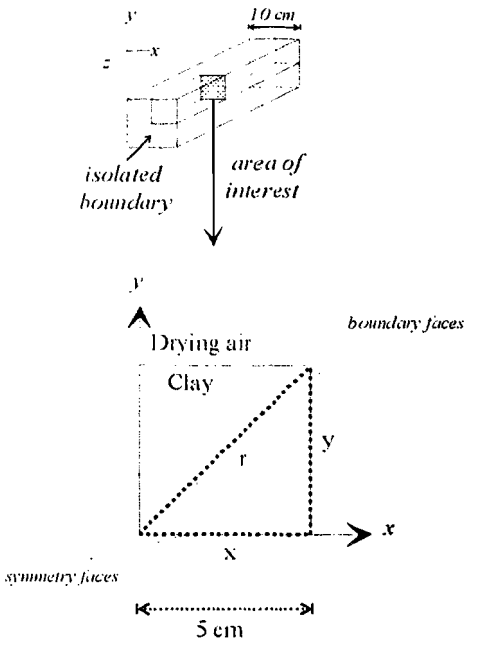

Fig. 4. Sample configuration and profiles of interest (r, x and y).

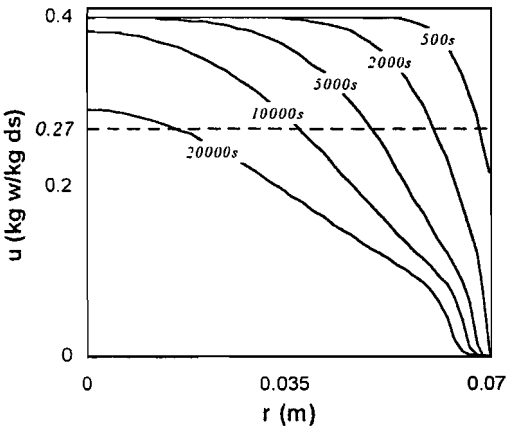

Fig. 5. Evolution of moisture content in the diagonal direction with space coordinate.

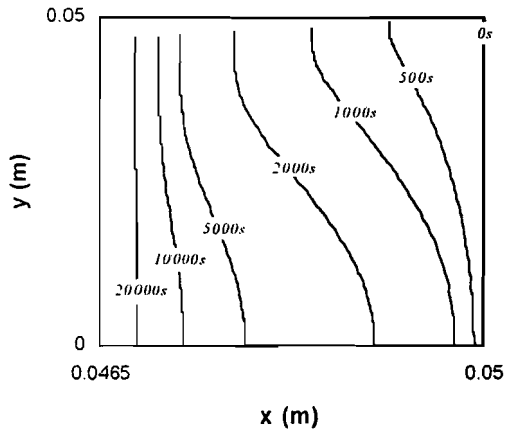

Fig. 6. Evolution of the external boundary surface y.

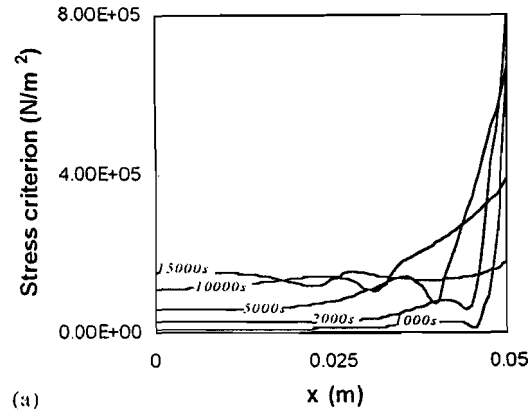

(a)

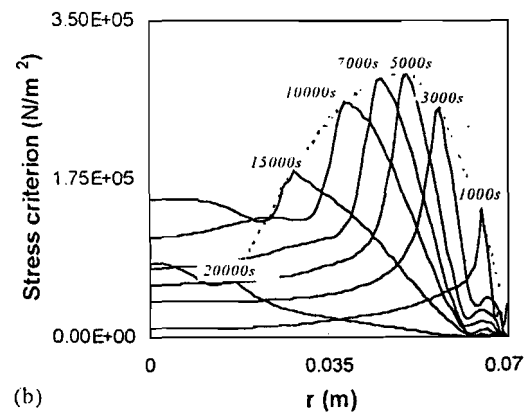

(b)

Fig. 7. Evolution of the stress criterion profile: (a) for the x direction; (b) for the r direction.

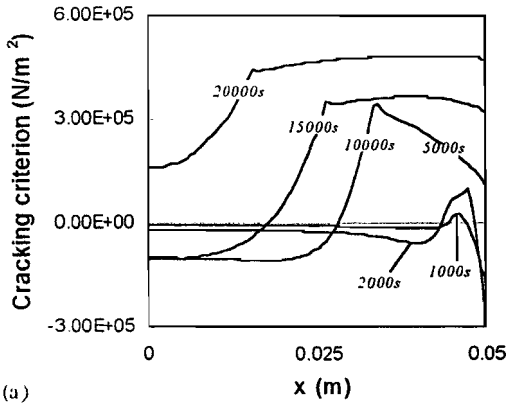

(a)

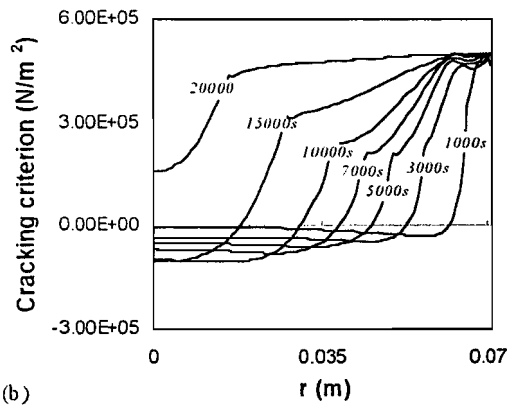

(b)

Fig. 8. Evolution of the cracking criterion profile: (a) for the x direction; (b) for the r direction.

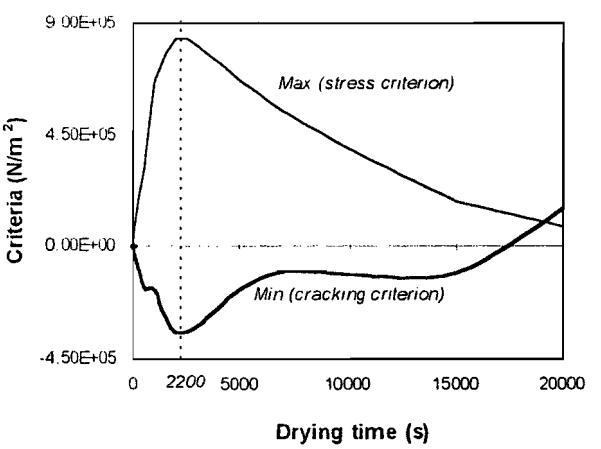

Fig. 9. Evolution of the stress criterion maximum and of the cracking criterion minimum for the global sample.

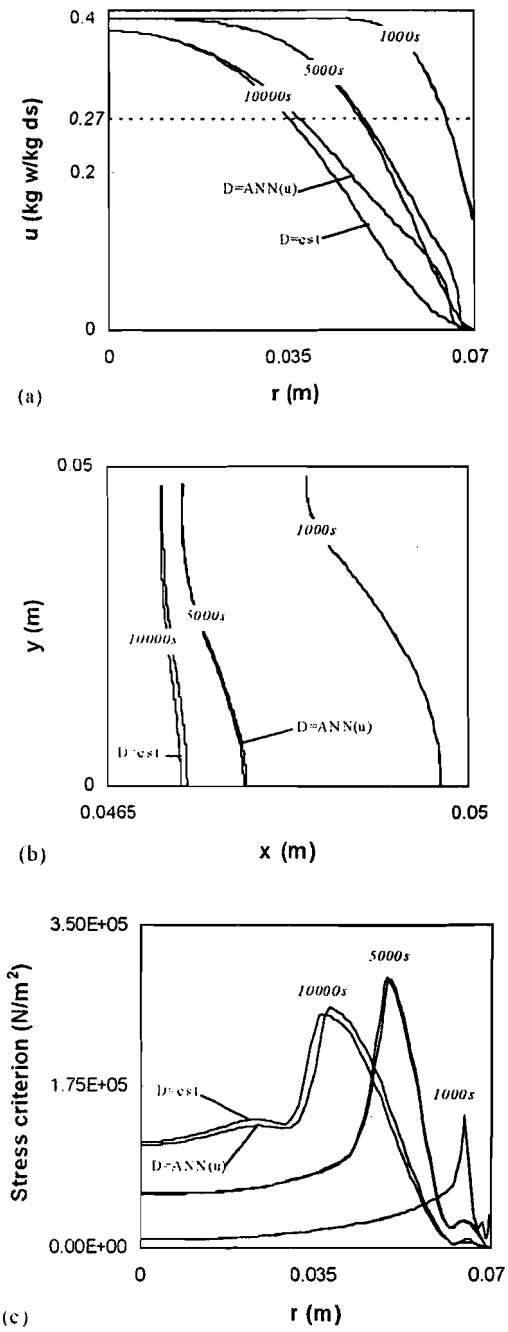

Fig. 10. Comparison of the effect of using D=ANN(u) and D=2.35 10^{-8} m^2s^{-1} on: (a) the moisture profile; (b) the displacement of the boundary; (c) the stress criterion.

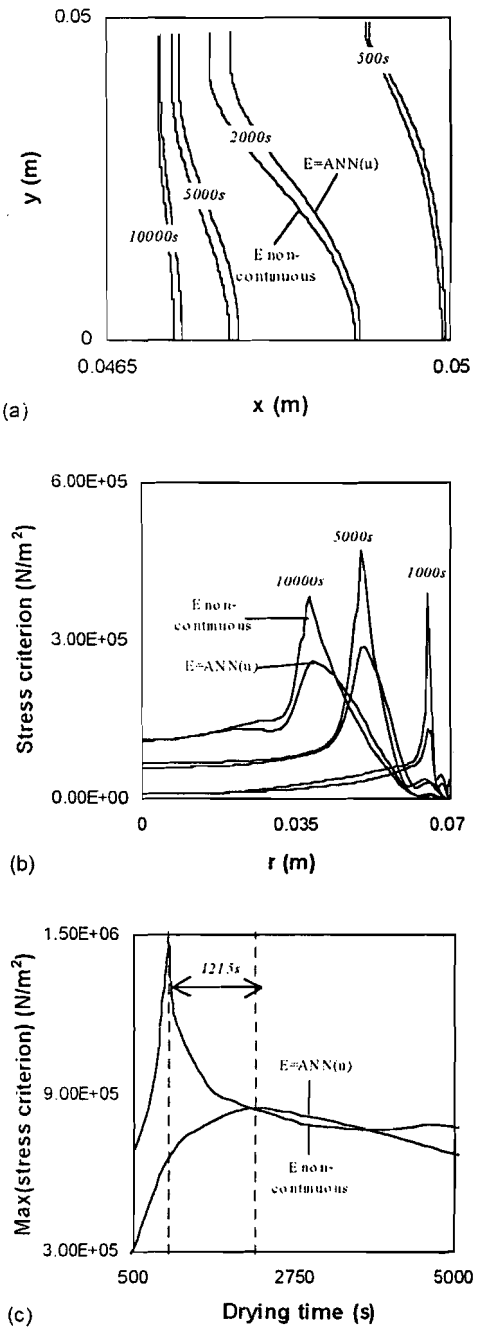

Fig. 11. Comparison of the effect of using a continuous and a non-continuous approximation of E on: (a) the displacement of the boundary; (b) the stress criterion; (c) the maximum of the stress criterion.